

Design and development of a charge cell for railway applications

Citation for published version (APA):

Verdenius, S. A., & Lopez Arteaga, I. (2014). *Design and development of a charge cell for railway applications*. (D&C; Vol. 2014.009). Eindhoven University of Technology.

Document status and date:

Published: 01/01/2014

Document Version:

Publisher's PDF, also known as Version of Record (includes final page, issue and volume numbers)

Please check the document version of this publication:

- A submitted manuscript is the version of the article upon submission and before peer-review. There can be important differences between the submitted version and the official published version of record. People interested in the research are advised to contact the author for the final version of the publication, or visit the DOI to the publisher's website.
- The final author version and the galley proof are versions of the publication after peer review.
- The final published version features the final layout of the paper including the volume, issue and page numbers.

[Link to publication](#)

General rights

Copyright and moral rights for the publications made accessible in the public portal are retained by the authors and/or other copyright owners and it is a condition of accessing publications that users recognise and abide by the legal requirements associated with these rights.

- Users may download and print one copy of any publication from the public portal for the purpose of private study or research.
- You may not further distribute the material or use it for any profit-making activity or commercial gain
- You may freely distribute the URL identifying the publication in the public portal.

If the publication is distributed under the terms of Article 25fa of the Dutch Copyright Act, indicated by the "Taverne" license above, please follow below link for the End User Agreement:

www.tue.nl/taverne

Take down policy

If you believe that this document breaches copyright please contact us at:

openaccess@tue.nl

providing details and we will investigate your claim.

Design and development of a charge cell for railway applications

S.A. Verdenius

DC 2014.009

Traineeship report

Coach: prof. dr. ir. L. Baeza (Universidad Politecnica Valencia, Valencia, Spain)

Supervisor: prof. dr. ir. I. Lopez Artega

Eindhoven University of Technology
Department of Mechanical Engineering
Dynamics and Control Group

Eindhoven, February, 2014

Abstract

The goal of this project is to design a new sensor to measure contact forces of train wheels with the track. This will be done in terms of a beam which will deform when a force by the wheel is applied. Due to the profile of the bottom of the train wheel, the shape of the beam is chosen to be cylindrical, with a smaller cylinder on top. The center of this small cylinder lies below the surface of the large cylinder to decrease the stress level. Also two cavities are created, one at each end of the beam, to allow constraints. The beam is dimensioned in such a way that the maximum stress in the beam does not exceed the Yield strength and that the maximum deflection is small enough.

When looking at a simply supported beam, the applied force in vertical direction is equal to the sum of the shear forces at the left and at the right of this applied force. To measure these shear forces, eight strains are registered. If one also wants to be able to measure forces applied under an angle, so considering a horizontal and a vertical force at the same time, sixteen strains need to be measured. Eight gauges are used and each gauge measures two strains, both under an angle of 45 degrees with the neutral axis. The gauges are placed on both ends of the horizontal and vertical neutral surface, at the left and right side of the applied force.

The forces can be applied at different z-positions on the small cylinder and under angles varying from 0 to π . To this end a grid is made and on these grid points, the relation between an applied force and all sixteen measured strains is determined, leading to sixteen equations. During a measurement the four unknowns, being the z-position, the angle, the force in vertical direction and the force in horizontal direction, are determined by minimizing the error in the sixteen known relations. When a force is not precisely exerted on a grid point, interpolation is used to solve the equations. This procedure is verified by simulations using ANSYS.

A sensitivity analysis showed that if all strains have the same percental error, this error can also be found in the calculated force. When all gauges have a different, normal distributed error, the error in the calculated forces is also normally distributed, with a standard deviation dependent on the size of the forces and linear dependent on the standard deviation of the error in the measured strains. The same conclusions can be drawn when there is no error in the strains, but an error in the grid. When both possible errors are combined, it turned out that if all errors are equal, they cancel out. If not, the error in the calculated forces is normally distributed with a standard deviation dependent on the sizes of the applied forces.

Finally the beam as described above is built and tested. Due to time reasons, only vertical forces are considered and thus only four gauges are used. To this end the Wheatstone bridge is applied and the theoretical linear relation between the output voltage and the applied force is determined. Experiments do show a linear relation, but with a slightly differing slope. Furthermore the experiments showed a different relationship when applying the force at a different location, while this is not the case in the theoretical model. This tells that there are still some errors in the placement of the gauges. Further examination can focus on eliminating this error and adding horizontal forces.

Contents

1	Problem description	4
2	Analytical relations	5
2.1	Relating the point load to shear force	5
2.2	Relating shear force to shear strain	7
2.3	Calculating applied forces through strain gauges	9
3	Design of the beam	11
3.1	Two-cylindrical shape of the beam	11
3.2	Dimensioning the beam	12
3.3	Additional requirements	14
4	Final algorithm	15
4.1	Applying a grid	15
4.2	Least square method	16
4.3	Alternative calculation using the method of Newton-Raphson	17
4.4	Simulation results	19
5	Sensitivity analysis	21
5.1	Error in measured strains	21
5.2	Error in grid	24
5.3	Combining errors	26
6	Experiments	27
6.1	Preparation of the beam	27
6.2	Wheatstone bridge	28
6.3	Calculate Force-Voltage curve	30
6.4	Results	31
7	Conclusion	35
A	Dimensions of the beam	36
B	Test data	38

1 Problem description

A new instrument for measuring contact forces of train wheels with the track needs to be designed. This instrument must be able to measure forces up to 20.000 Newton. It needs to measure forces that are applied under an angle and at different positions. The instrument must be able to measure at as much points along the bottom of the train wheel as possible. To this end a beam will be designed, which will deform when forces are applied. These deformations will be registered and through these deformations, the applied force can be retrieved.

The instrument must be designed and algorithms should be provided to calculate the applied force. This all must be verified using simulations with ANSYS and by using a real test set-up. Furthermore a sensitivity analysis must be made.

2 Analytical relations

To measure deformations when a force is applied on the beam, strain gauges will be used. Strain gauges can be placed along a beam and can measure the local strain. This shear strain can be related to shear force, which can then be related to the applied force. First of all, these analytical relationships must be found.

2.1 Relating the point load to shear force

Consider a simply supported beam of length L as depicted in figure 1. For simplicity, we first assume only one vertical point load is exerted. This point load, P , acts somewhere on the beam, indicated by distances a and b . The beam is constrained in its utmost left node in all three degrees of freedom, while the right end can still freely move in one direction.

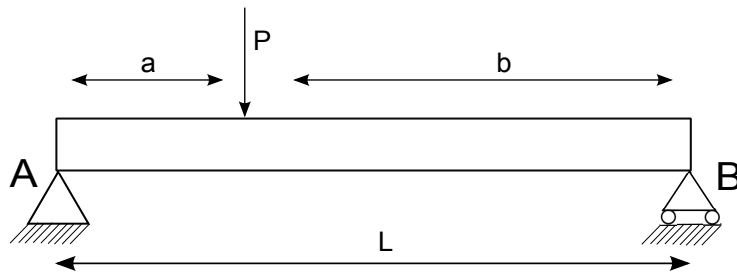


Figure 1: A simply supported beam

To calculate the shear forces at any section of the beam, the reaction forces in nodes A and B need to be known. These forces can be found by using two equations for equilibrium, being the equilibrium of moments and the equilibrium of forces in y -direction:

$$\sum M = 0 \quad (1)$$

and

$$\sum F_y = 0. \quad (2)$$

For the situation of figure 1, equation 1 can be written into the following two equations:

$$\sum M_A = Pa - R_B L = 0 \quad (3)$$

and

$$\sum M_B = -Pb + R_A L = 0. \quad (4)$$

Using the same analogy, equation 2 becomes

$$\sum F = R_A + R_B - P = 0. \quad (5)$$

Here R_A and R_B indicate the reaction forces in the left and right support respectively, both pointed upwards. With only R_A and R_B as unknowns, this problem can be solved, leading to the following expressions for the reaction forces:

$$R_A = Pb/L \quad (6)$$

and

$$R_B = Pa/L. \quad (7)$$

How these forces are related to the shear force V can be seen when cutting a piece from the beam, as done in figure 2.

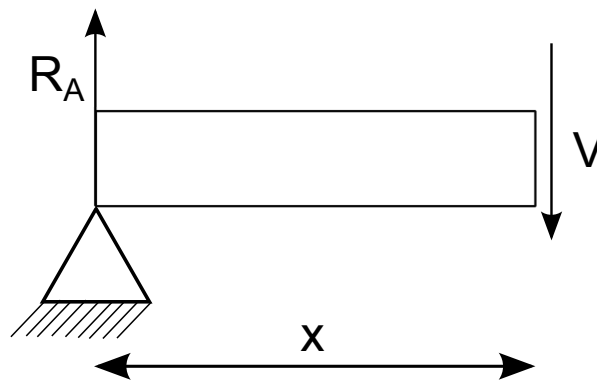


Figure 2: A beam cut in half

The variable x indicates the distance from the left support to the place where the shear force is measured. When x is smaller than a , we get the situation of figure 2. Again, the sum of the forces in y -direction needs to be zero, so the shear force at the left side of the point load must be equal to R_A , so Pb/L . From similar calculations the conclusion can be drawn that the shear force at the right side of the point load, so when x is larger than a , is equal to $-Pa/L$. The total force can then be found by adding the shear force at the left and right side of the point load. This all is depicted in figure 3.

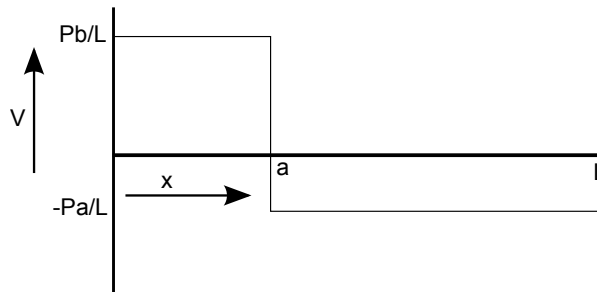


Figure 3: The shear force diagram

2.2 Relating shear force to shear strain

The shear force as described in the previous section can be related to the shear stress. According to [3], these quantities are coupled via the following equation:

$$\tau = VQ/Ib. \quad (8)$$

In this equation τ is the shear stress, V the shear force, Q the first moment of area, I the moment of inertia and b is the width of the beam.

The width of the beam, the first moment of area and the moment of inertia are dependent on the shape of the beam. For the situations in which this beam will be used, a circular beam is most practical. This will be explained further on in this report. For a circular beam, [3] states that the moment of inertia is equal to

$$I = \frac{\pi}{4}R^4. \quad (9)$$

To calculate the first moment of area, first the point of measurement needs to be determined. For the best results one must measure strains at the place where they are the highest. This is at the neutral axis of a beam, the plane through the center of the cylinder. The first moment of area can then be defined as the area above the neutral axis multiplied with the distance from the centroid of this area to the neutral axis. This is also depicted in figure 4.

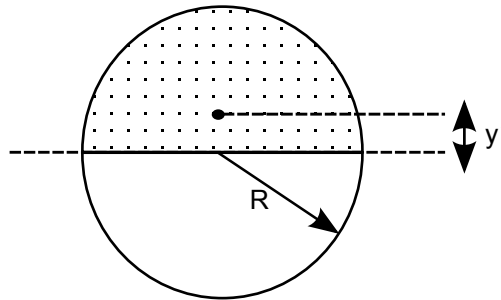


Figure 4: How to determine the first moment of area

Captured in formulas this becomes

$$Q = \frac{1}{2}\pi R^2 y', \quad (10)$$

where [3] states that

$$y' = \frac{4}{3\pi}R. \quad (11)$$

Combining these equations leads to one expression for the moment of area:

$$Q = \frac{2}{3}R^3. \quad (12)$$

By using our expressions for Q,I and b, equation 8 can be simplified to

$$V = \frac{3}{4}\tau A. \quad (13)$$

This way the shear stress is directly related to the shear force (and thus the point load). One extra step is needed, since our gauges measure strain, not stress. The shear strain γ and shear stress τ are coupled through one formula, being

$$\gamma = \tau/G. \quad (14)$$

Here G is the shear modulus. This constant is material dependent and can be calculated using Youngs modulus E and Poisson ratio ν in the following way:

$$G = \frac{E}{2(1 + \nu)}. \quad (15)$$

To find the shear strain γ , three strains under an angle of 45 degrees need to be measured, as illustrated in figure 5.

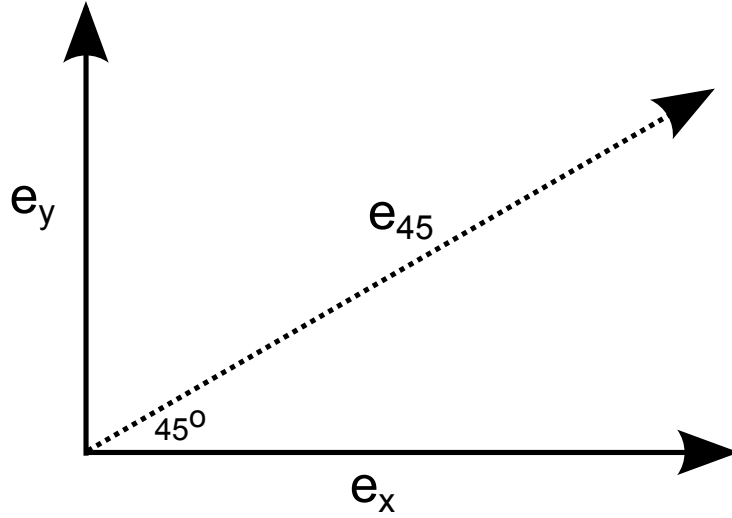


Figure 5: Depiction of the three strains that need to be measured

Here e_x and e_y represent the strain in x- and y-direction respectively. The third arrow, e_{45} , represents the strain measured under an angle of 45 degrees. When these three strains are known, the shear strain γ_{xy} can be calculated using

$$\gamma_{xy} = 2e_{45} - (e_x + e_y). \quad (16)$$

However, simulations showed that the strains in x- and y-direction are so small compared to the strain under an angle of 45 degrees, that they can be omitted.

All equations from this section can then be combined into one single equation, being

$$V = \frac{3}{2}AGe_{45}. \quad (17)$$

This way the shear force in any part of the beam can be found by looking at the strain under an angle of 45 degrees in that part.

2.3 Calculating applied forces through strain gauges

The force which will be exerted by the train wheel will not necessary touch the beam exactly in the middle. As seen earlier in this section, the force can thus be determined by adding the shear force at the left and right of the applied force. In the next picture, the beam is cut in half. On each part two strain gauges are placed, which each measure two strains under an angle of 45 degrees:

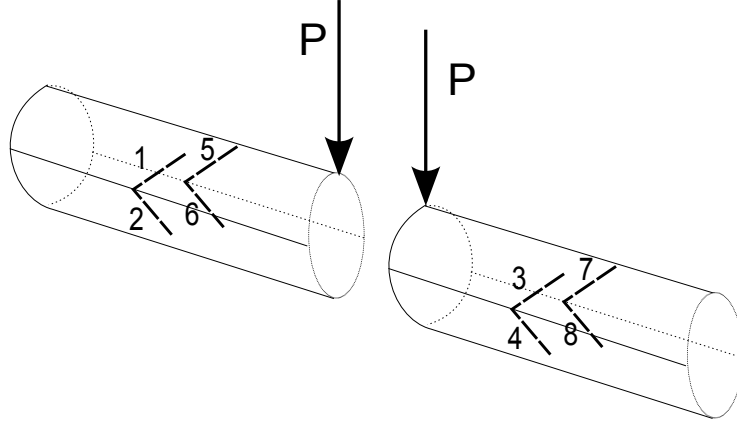


Figure 6: Beam with four strain gauges, cut in half

All strain gauges are placed on the neutral axis in such a way that they measure two strains which are both under an angle of 45 degrees with this axis. Two gauges are placed on one end of the neutral surface, the other two are placed on the other end of the neutral surface. According to [5], the shear strain in the left configuration is equal to

$$\gamma_{left} = e_1 + e_5 - e_2 - e_6. \quad (18)$$

The shear strain in the right side, which is in the same configuration, but then mirrored, can be expressed in a similar way as

$$\gamma_{right} = e_8 + e_4 - e_7 - e_3. \quad (19)$$

Since the total force can be found by adding both shear forces and knowing there is a linear relation between shear strain and shear force, one can say that

$$P \sim e_1 + e_4 + e_5 + e_8 - e_2 - e_3 - e_6 - e_7. \quad (20)$$

In our experiment also a horizontal force will occur. A horizontal force can be compared with the current situation, but then rotated for ninety degrees. That is why four more strain gauges are added, this time on the vertical neutral axis. These gauges, measuring strains e_9 to e_{16} , are added in a similar order as in the picture above. One can thus conclude that when applying only a horizontal force Q , this force is linearly related to the strains in the following way:

$$Q \sim e_9 + e_{12} + e_{13} + e_{16} - e_{10} - e_{11} - e_{14} - e_{15}. \quad (21)$$

The way these strains are related to the exerted force, depends on where the force is applied. This will be discussed in a next section. First the complete design of the beam is discussed.

3 Design of the beam

The beam must be designed in such a way that forces at different positions of the train wheel can be measured. That is why one must take into account the shape of the train wheel. Furthermore some overall requirements must be met, such as the maximum stress and the maximum deflection of the beam.

3.1 Two-cylindrical shape of the beam

Where a normal cylinder has an equal radius along its length, a train wheel has a varying diameter. This is necessary for trains to stay on the track. The bottom of a trainwheel is thus not flat, as can be seen in figure 7, where a standard wheelset of a train is depicted. The dashed circle is not a part of the wheel set.

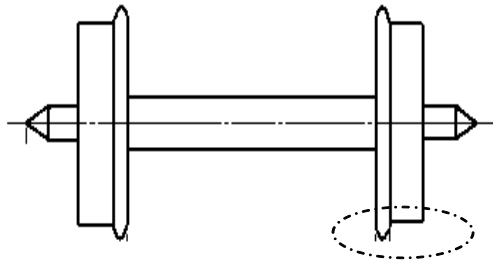


Figure 7: Front view of a wheelset of a train

As can be seen, the radius is the smallest on the outside of the train. For determining the shape of the beam, this bottom profile of the train wheel is of importance. That is why this bottom profile is modeled and for the right wheel of figure 7, the bottom profile in the dashed circle is depicted in more detail in figure 8.

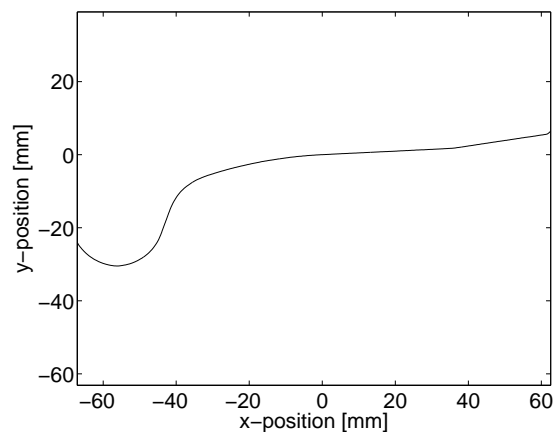


Figure 8: Profile of the bottom of the train wheel

Looking at this picture, a rectangular beam can immediately be eliminated. Using a rectangular beam, the force will never be applied on the top of the beam. A circular beam is a better choice. Since the beam must be able to measure at all x-positions along the bottom surface of the train wheel, a circular beam with a small radius is needed, so it can also measure in the curve around the x-position of 40 mm.

A circular beam with a small diameter however is not ideal. That is why the choice is made for a circular beam with a bigger diameter, which has a smaller cylinder added on top. This way forces can be measured at almost every x-position along the bottom of the wheel and the force only has a small surface of contact with the beam. This is depicted below in figure 9.

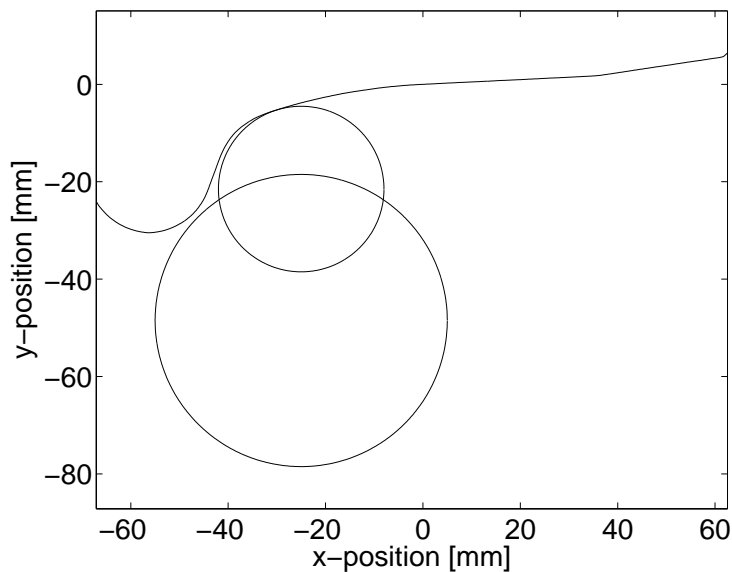


Figure 9: Profile of the train wheel with the two-cylindrical design of the beam

3.2 Dimensioning the beam

The first question that must be answered is how the beam will be constrained. Until this point a simply supported beam was assumed, but when applying both horizontal and vertical forces, this is not possible anymore. That is why the large cylinder is modeled with two cavities, one at each end of the beam. By making cavities, the cylinder has a flat bottom surface at each end, which can then be constrained in all degrees of freedom. In reality the beam will be constrained by attaching this flat surface to the fixed world, using a screw that goes from the bottom of the cavity to the neutral axis. These cavities can be seen in the design of the beam in figure 10.

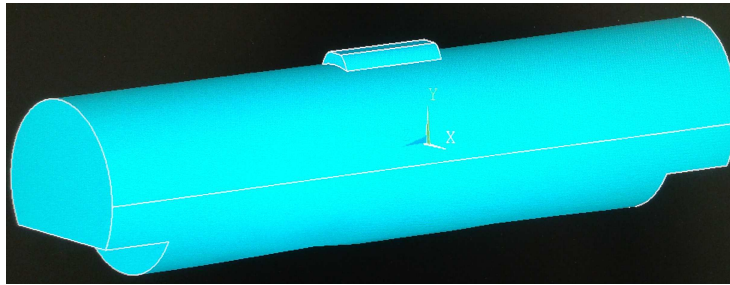


Figure 10: Illustration of the cavities needed to constrain the beam

The criterion for choosing dimensions is that the beam can measure the largest range of positions along the wheel. Besides of that, high strains are required for the best measurement results. However, at all times the maximum stress must be lower than the Yield strength and the deflections must be small enough.

First the radius and length of the large beam are determined. Models are made with a radius of 0.03 meter, 0.04 meter and 0.05 meter. The length is varied from 0.4 to 0.8 meters. The final design is a cylinder with a length of 0.4 meters and a radius of 0.03 meters. Varying the dimensions of the small cylinder turned out to have little influence on the occurring stresses and strains. The length is varied from 0.06 to 0.1 meters and the radius from 0.01 to 0.02 meters. Since the dimensions had little influence, the design is chosen in which the small cylinder fits the train wheel the best and has the smallest length. The final dimensions are determined to be a length of 0.06 meters and a radius of 0.017 meters.

The depth of the cavities is varied between 0.0075 and 0.015 meters and the conclusion is that the best results are retrieved when the cavities are the deepest. However, 0.015 meters is considered as maximum depth to save the shape of a cylinder. Also the width of the cavities is varied between 0.04 and 0.06 meters. The best results were retrieved with the smallest cavities. That is why the cavities finally have a width of 0.04 meters and a depth of 0.0075 meters.

The center of the small cylinder is not on top of the large cylinder, but a bit lower. It turned out that the lower the center is, the lower the stresses are that occur. However, to have a large enough surface to apply a force on, the center cannot be too low. That is why the center is placed at a distance of 2.7 centimeters from the center of the large cylinder.

With these dimensions one can measure almost everywhere along the bottom of the wheel. All dimensions can be found in appendix A.

3.3 Additional requirements

As shortly mentioned above, the stresses that occur must always be lower than the Yield strength, to prevent the beam from going into the range of plastic deformation. Calculations regarding the stresses in the beam when applying a point load can be made by hand. These stresses are the highest in the bottom fibers and according to [3], for a simply supported beam they can be found using

$$\sigma = \frac{Mz}{I}. \quad (22)$$

Here z represents the distance from the neutral axis to the point of measurement of the stress, so in our case $z=r$. I is again the moment of inertia, being $\frac{\pi}{4}R^4$. As stated in [3], the moment for a simply supported beam is equal to

$$M = \frac{Pl}{4}. \quad (23)$$

The maximum stress in the beam is thus equal to

$$\sigma = \frac{Pl}{\pi R^3}. \quad (24)$$

When neglecting the small cylinder on top and assuming one only wants to measure vertical forces up to 20.000 Newton, the material must have a Yield strength of 95 MPa or higher. Using Ansys, the maximum stress found in the beam when applying a vertical force of 20.000 Newton is 105 MPa. This difference is likely due to the adaption of the beam with cavities and a small cylinder.

Furthermore attention must be paid to the maximum deflection of the beam. In previous calculations the x- and y-directions are stated, but these directions will change due to the deflection of the beam. However, as can be found in [3], the maximum angle due to deflection is equal to $-\frac{0.0642l^2}{EI}P$. In a similar way, the maximum deflection in y-direction is equal to $-\frac{l^2}{48EI}P$. When designing the beam, one must take into account that these deflections stay small. If the dimensions as stated above are used, the maximum angle and deflection will be -0.0015 radians and $-4.99e^{-4}$ meter respectively, when applying a force of 20.000 Newton.

4 Final algorithm

The beams dimensions are determined and the position of the strain gauges is known. Earlier the conclusion is made that sixteen strains are sufficient to determine the applied forces. This section will describe the method to determine these applied forces.

4.1 Applying a grid

When looking back at figure 9, one can see that the force from the train wheel will not be applied completely vertical or completely horizontal on the beam, but that it will be applied under an angle. For the ease of calculations, this force will be split into a vertical and horizontal force. Furthermore, for each new measurement at a different position along the bottom of the train wheel, the point where this force acts on the beam may be different. This influences the measured strains. That is why the place where these forces F_x and F_y are applied on the beam needs to be taken into account. Hereto this point is defined by angle α and distance z as depicted below:

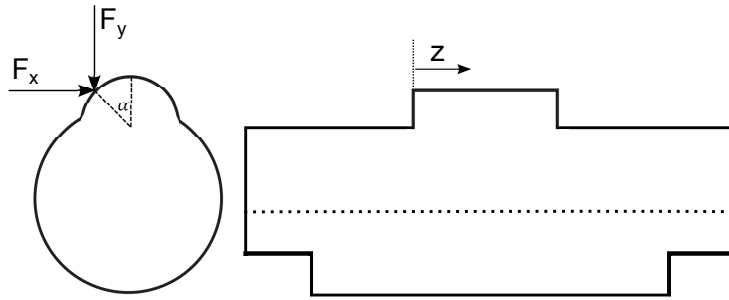


Figure 11: Front and side view of the beam with definitions of variables

From figure 9 it can be concluded that forces can be exerted on a quarter of the outer surface of the small cylinder. On this surface a grid is made of elements of equal size. They differ in z - and α -position as depicted in the next figure.

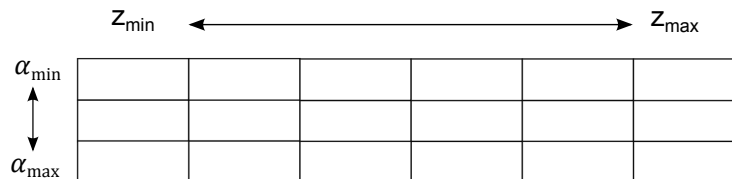


Figure 12: Illustration of grid applied on small cylinder

As determined earlier, a combination of strains is linearly related to the shear force. The relations presented earlier are only exactly correct if there is only a horizontal or vertical force and if this force is applied at the middle of the beam at $\alpha = 0$. To examine what the relation is in case of combined forces which are applied at a different place, each of the sixteen strains is observed individually.

When applying a horizontal force of 1 Newton on one of the grid points with coordinates z_i and α_j , sixteen strains are registered. These strains are called $C_{1x}(z_i, \alpha_j)$ to $C_{16x}(z_i, \alpha_j)$. The same is done when applying a vertical force of -1 Newton, leading to strains $C_{1y}(z_i, \alpha_j)$ to $C_{16y}(z_i, \alpha_j)$. The strain when applying both a horizontal and vertical force is the sum of both individual strains. This leads to the following matrix equation for grid point z_i, α_j :

$$\begin{pmatrix} e_1 \\ e_2 \\ \vdots \\ e_{16} \end{pmatrix} = \begin{pmatrix} C_{1x}(z_i, \alpha_j) & C_{1y}(z_i, \alpha_j) \\ C_{2x}(z_i, \alpha_j) & C_{2y}(z_i, \alpha_j) \\ \vdots & \vdots \\ C_{16x}(z_i, \alpha_j) & C_{16y}(z_i, \alpha_j) \end{pmatrix} \begin{pmatrix} F_x \\ F_y \end{pmatrix}. \quad (25)$$

To be able to calculate forces at all grid points, the coefficients in the middle matrix are determined for $z=0, 0.01, \dots, 0.06$ and $\alpha=0, \frac{1}{8}\pi, \dots, \frac{1}{2}\pi$. By rewriting this equation, one can calculate the applied forces from the measured strains, if the coefficients are known (that is: if the forces are applied on a grid point). The equation for this is

$$\begin{pmatrix} F_x \\ F_y \end{pmatrix} = (C^T C)^{-1} C^T e. \quad (26)$$

Here e is the column with all sixteen strains (16x1) and C is the middle matrix from equation 25, holding all coefficients C_{kl} for a certain z and α (16x2). Note that this method only works when z and α are known. When one wants to measure at a point which is not exactly a grid point, the values of coefficients C_{kl} are determined by interpolation, using the values of coefficients C_{kl} from the surrounding grid points.

4.2 Least square method

A problem occurs when z and α are unknown, which is the case in our real test set-up. Since the coefficients C_{kl} depend on z and α , our problem has four unknowns. The easiest way of solving this problem is using the least square method.

To this end, equation 25 is rewritten into sixteen individual equations which all must be equal to 0:

$$\begin{aligned} e_1 - C_{1x}(z, \alpha)F_x - C_{1y}(z, \alpha)F_y &= 0 \\ e_2 - C_{2x}(z, \alpha)F_x - C_{2y}(z, \alpha)F_y &= 0 \\ &\vdots \\ e_{16} - C_{16x}(z, \alpha)F_x - C_{16y}(z, \alpha)F_y &= 0. \end{aligned} \quad (27)$$

In an experiment, all sixteen strains are measured and thus known. The four unknowns must be chosen such that all equations are zero. Since it will be hard to find coefficients for which all equations are exactly 0, one must try to bring all equations as close to zero as possible. This is done by introducing Γ_i , which is defined as

$$\Gamma_i = (e_i - C_{ix}(z, \alpha)F_x - C_{iy}(z, \alpha)F_y)^2. \quad (28)$$

The best solution is found when all equations are close to zero. That is why we want to minimize

$$\sum_{i=1}^{16} \Gamma_i \quad (29)$$

for all unknowns. This can be done using Matlabs function 'minimize' and Matlab then returns the values for z, α, F_x and F_y for which equation 29 is minimized:

$$\min(z, \alpha, F_x, F_y) \sum_{i=1}^{16} \Gamma_i. \quad (30)$$

As an initial guess for z and α one must choose values corresponding to the situation of testing. As initial guesses for F_x and F_y the formulas are used with which they could be determined if there was only a vertical or only a horizontal load applied at the middle of the beam, being

$$F_x = \frac{e_9 + e_{12} + e_{13} + e_{16} - e_{10} - e_{11} - e_{14} - e_{15}}{C_{9x} + C_{12x} + C_{13x} + C_{16x} - C_{10x} - C_{11x} - C_{14x} - C_{15x}} \quad (31)$$

and

$$F_y = \frac{e_1 + e_4 + e_5 + e_8 - e_2 - e_3 - e_6 - e_7}{C_{1y} + C_{4y} + C_{5y} + C_{8y} - C_{2y} - C_{3y} - C_{6y} - C_{7y}}, \quad (32)$$

where the coefficients of C are thus based on $z = 0.03$ and $\alpha = 0$.

4.3 Alternative calculation using the method of Newton-Raphson

Another way of solving this problem is using the method of Newton-Raphson with four equations. The first two equations can be built from equation 26. When defining the matrix $(C^T C)^{-1} C^T$ as matrix D, the equation can be rewritten into

$$\begin{pmatrix} F_x \\ F_y \end{pmatrix} = \begin{pmatrix} D_{1,1}(z, \alpha) & D_{1,2}(z, \alpha) & \cdots & D_{1,16}(z, \alpha) \\ D_{2,1}(z, \alpha) & D_{2,2}(z, \alpha) & \cdots & D_{2,16}(z, \alpha) \end{pmatrix} \begin{pmatrix} e_1 \\ e_2 \\ \vdots \\ e_{16} \end{pmatrix}, \quad (33)$$

which can then be split into two individual equations, being

$$F_x = (D_{1,1}(z, \alpha) \quad D_{1,2}(z, \alpha) \quad \cdots \quad D_{1,16}(z, \alpha)) \begin{pmatrix} e_1 \\ e_2 \\ \vdots \\ e_{16} \end{pmatrix} \quad (34)$$

$$F_y = (D_{2,1}(z, \alpha) \quad D_{2,2}(z, \alpha) \quad \cdots \quad D_{2,16}(z, \alpha)) \begin{pmatrix} e_1 \\ e_2 \\ \vdots \\ e_{16} \end{pmatrix}. \quad (35)$$

The third equation can be found by combining the strains in the horizontal neutral plane, as discussed earlier. The following relation namely holds:

$$ee_3 = (CC_{3x}(z, \alpha) \quad CC_{3y}(z, \alpha)) \begin{pmatrix} F_x \\ F_y \end{pmatrix}, \quad (36)$$

where

$$\begin{aligned} ee_3 &= e_1 + e_4 + e_5 + e_8 - e_2 - e_3 - e_6 - e_7, \\ CC_{3x}(z, \alpha) &= C_{1x}(z, \alpha) + C_{4x}(z, \alpha) + C_{5x}(z, \alpha) + C_{8x}(z, \alpha) - \\ &\quad C_{2x}(z, \alpha) - C_{3x}(z, \alpha) - C_{6x}(z, \alpha) - C_{7x}(z, \alpha), \end{aligned}$$

and

$$\begin{aligned} CC_{3y}(z, \alpha) &= C_{1y}(z, \alpha) + C_{4y}(z, \alpha) + C_{5y}(z, \alpha) + C_{8y}(z, \alpha) - \\ &\quad C_{2y}(z, \alpha) - C_{3y}(z, \alpha) - C_{6y}(z, \alpha) - C_{7y}(z, \alpha). \end{aligned}$$

A similar equation can be formulated with the eight strains in the vertical neutral plane, being

$$ee_4 = (CC_{4x}(z, \alpha) \quad CC_{4y}(z, \alpha)) \begin{pmatrix} F_x \\ F_y \end{pmatrix}, \quad (37)$$

where

$$\begin{aligned} ee_4 &= e_9 + e_{12} + e_{13} + e_{16} - e_{10} - e_{11} - e_{14} - e_{15}, \\ CC_{4x}(z, \alpha) &= C_{9x}(z, \alpha) + C_{12x}(z, \alpha) + C_{13x}(z, \alpha) + C_{16x}(z, \alpha) - \\ &\quad C_{10x}(z, \alpha) - C_{11x}(z, \alpha) - C_{14x}(z, \alpha) - C_{15x}(z, \alpha), \end{aligned}$$

and

$$\begin{aligned} CC_{4y}(z, \alpha) &= C_{9y}(z, \alpha) + C_{12y}(z, \alpha) + C_{13y}(z, \alpha) + C_{16y}(z, \alpha) - \\ &\quad C_{10y}(z, \alpha) - C_{11y}(z, \alpha) - C_{14y}(z, \alpha) - C_{15y}(z, \alpha). \end{aligned}$$

In this way four equations result which are only dependent on four unknowns.

To use the method of Newton-Raphson, the four unknowns will be placed in a single matrix, being $x = (z, \alpha, F_x, F_y)$. Furthermore the four equations need to be defined in the form of $\varphi_i = 0$. This results in:

$$\varphi_1 = (D_{1,1}(x_1, x_2) \quad D_{1,2}(x_1, x_2) \quad \cdots \quad D_{1,16}(x_1, x_2)) \begin{pmatrix} e_1 \\ e_2 \\ \vdots \\ e_{16} \end{pmatrix} - x_3 \quad (38)$$

$$\varphi_2 = (D_{2,1}(x_1, x_2) \quad D_{2,2}(x_1, x_2) \quad \cdots \quad D_{2,16}(x_1, x_2)) \begin{pmatrix} e_1 \\ e_2 \\ \vdots \\ e_{16} \end{pmatrix} - x_4 \quad (39)$$

$$\varphi_3 = ee_3 - (CC_{3x}(x_1, x_2) \quad CC_{3y}(x_1, x_2)) \begin{pmatrix} x_3 \\ x_4 \end{pmatrix} \quad (40)$$

$$\varphi_4 = ee_4 - (CC_{4x}(x_1, x_2) \quad CC_{4y}(x_1, x_2)) \begin{pmatrix} x_3 \\ x_4 \end{pmatrix}. \quad (41)$$

With these definitions we can state the method of Newton-Raphson, which will make x converge to a constant value, where expressions φ_1 to φ_4 are approximately zero. This algorithm is stated as follows:

$$x_{k+1} = -[J]^{-1}\varphi(x_k) + x_k. \quad (42)$$

Here φ is the column of expressions φ_1 to φ_4 and J denotes the Jacobian of matrix φ . The Jacobian is defined as follows:

$$J = \begin{pmatrix} \frac{\delta\varphi_1}{\delta x_1} & \dots & \frac{\delta\varphi_1}{\delta x_4} \\ \vdots & \ddots & \vdots \\ \frac{\delta\varphi_4}{\delta x_1} & \dots & \frac{\delta\varphi_4}{\delta x_4} \end{pmatrix}. \quad (43)$$

Since we are working with numerical expressions, derivatives are approximated in the following way:

$$\frac{\delta\varphi_i}{\delta x_j} = \frac{\varphi_i(x + \delta x_j) - \varphi_i(x)}{\delta x_j}, \quad (44)$$

where δx_j must be chosen small enough.

The iteration procedure then consists of the following four steps:

1. Make a guess for the initial value of x . The first two values, being z and α , can be estimated accurate, since by experimenting it is clear around which point the forces are applied. The initial values for F_x and F_y are determined in the same way as described in section 4.2.
2. Using these values for x , matrix φ is calculated. If the values of z and α are not equal to those of a grid point, the values for C_{ij} at this point are determined through interpolation from the closest grid points.
3. After solving equation 42, we retrieve a new value for matrix x , which then will be used as input for a new iteration.
4. Steps 2 and 3 are repeated until x is converged, that is when $|x_{k+1} - x_k| < 1e^{-4}$.

4.4 Simulation results

Using both procedures, a few simulations are done with our model in ANSYS. A combination of a horizontal and vertical force is applied and the sixteen strains are registered. After this, the applied force is calculated from these sixteen strains using both procedures as described above. In the tables below the results can be found of ten measurements. A random combination of forces is applied at a random point on the beam. However, in the first five tests, the forces are applied at a grid point. In the latter five, this is not the case and the results are based on interpolation.

Table 1: Simulation results for calculating F_x

	F_x applied	F_x measured least square	F_x measured Newton
Test 1	4.0000 N	3.9999 N	3.9999 N
Test 2	2.0000 N	2.0000 N	1.9999 N
Test 3	3.0000 N	3.0000 N	3.0000 N
Test 4	5.0000 N	5.0000 N	5.0000 N
Test 5	4.0000 N	4.0000 N	4.0000 N
Test 6	4.0000 N	4.0002 N	4.0001 N
Test 7	2.0000 N	2.0005 N	2.0001 N
Test 8	3.0000 N	3.0001 N	3.0001 N
Test 9	5.0000 N	5.0004 N	5.0000 N
Test 10	4.0000 N	4.0000 N	4.0000 N

Table 2: Simulation results for calculating F_y

	F_y applied	F_y measured least square	F_y measured Newton
Test 1	10.0000 N	10.0000 N	10.0000 N
Test 2	8.0000 N	8.0000 N	7.9999 N
Test 3	7.0000 N	7.0001 N	7.0001 N
Test 4	5.0000 N	5.0000 N	5.0000 N
Test 5	9.0000 N	8.9999 N	8.9999 N
Test 6	10.0000 N	10.0017 N	10.0000 N
Test 7	8.0000 N	8.0026 N	8.0000 N
Test 8	7.0000 N	7.0002 N	7.0000 N
Test 9	5.0000 N	5.0004 N	5.0000 N
Test 10	9.0000 N	9.0022 N	9.0002 N

All measured forces are close to the actual forces. When applying a force on a grid point, the maximum error is only 0.0001 Newton. When using interpolations, the errors are a bit bigger. However, for the Newton-Raphson method these errors are within the tolerance set by the user.

When looking only at this table, one must conclude that using the method of Newton-Raphson leads to the best results. A big advantage of the least-square method is that it always gives a result. The Newton-Raphson method only gives a result if the initial values for z and α are close to their real values. Since these values can be guessed quite accurate when performing tests, this is not a big problem.

Assuming the z -position can be estimated with an accuracy of ± 0.01 meters and that angle α can be determined with an accuracy of ± 0.2 radians, also conclusions can be drawn on the computing time. Taking the worst-case scenario, the least-square method can take up to 4.22 seconds to compute the forces, whereas the method of Newton-Raphson converges within 0.39 seconds.

5 Sensitivity analysis

The calculations in the previous section are all based on the assumption that the strain gauges can measure strain accurate up to 4 digits. However, in reality this is of course not the case. There will be some errors in the measurements. To check how this influences the final results, this section will focus on the sensitivity of our instruments.

5.1 Error in measured strains

First of all we assume that our model completely corresponds to the real test set-up. This means that the values of the grid are correct. However, an error is applied to the measured strains, since this is most likely to occur. Since the forces are based on these strains, an error in the strain will definitely lead to an error in the calculated force. To check this, the following experiment is done.

First, a random position and force is chosen. With the formulas derived earlier (equation 25), the corresponding strains will be determined. After this, all strains will be given the same percental error. This is done by multiplying the strain with δ , where δ is defined as $1+N(0,p/100)$. This last term indicates a Gaussian distribution with an average value of zero and a standard deviation of percentage p . In our experiments, this percentage will be 1,2 and 4.

When all strains are multiplied with this value, both procedures of chapter 4 are used to calculate the applied forces. Since the exact applied forces are known, one can determine the error in the calculated forces. For a fixed percentage p , this procedure is repeated 2000 times. This way the errors in the strains will follow a normal distribution. Since also 2000 errors in both forces are calculated, one can check if these also follow a normal distribution.

As an example, below the distributions are shown when using the least square method and a percentage of 2%. The error in the strain can be seen in figure 13. As expected, both F_x (figure 14) and F_y (figure 15) follow the same distribution.

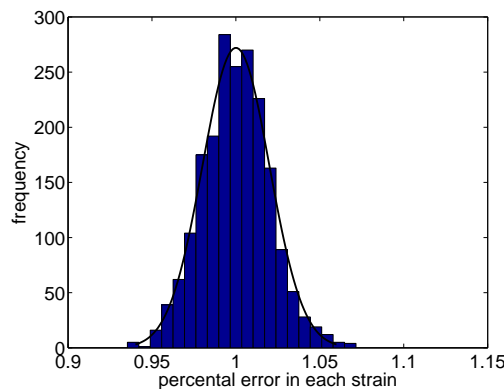
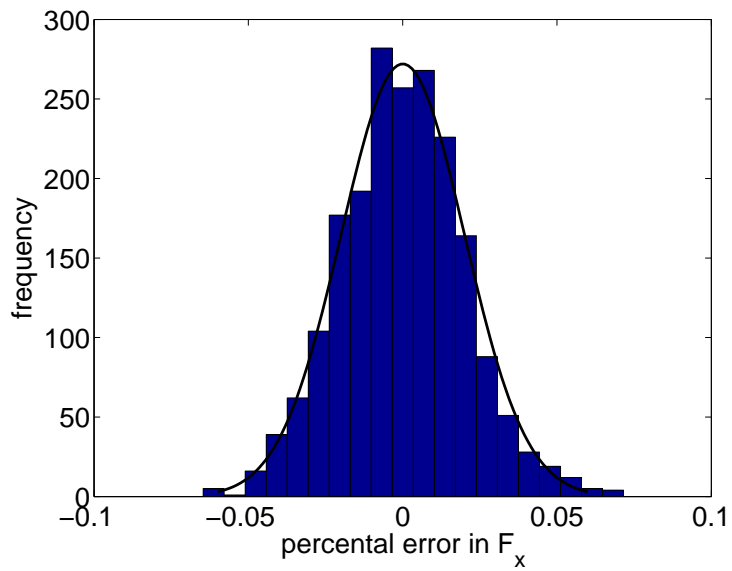
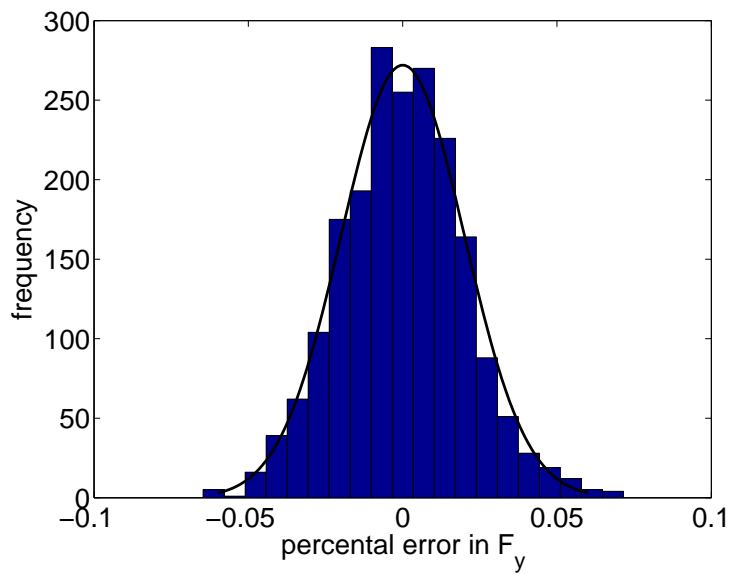


Figure 13: Normal distributed error in strains

Figure 14: Normal distributed error in F_x Figure 15: Normal distributed error in F_y

When repeating the same procedure for standard deviations of 1% and 4%, the following table with the results of both procedures can be created.

Table 3: Standard deviations of errors for an equal error in all strains

$\sigma(\text{error } e)$	$\sigma(\text{error } F_x)$ Least square	$\sigma(\text{error } F_y)$ Least square	$\sigma(\text{error } F_x)$ Newton-Rap.	$\sigma(\text{error } F_y)$ Newton-Rap.
0.0090	0.0090	0.0090	0.0090	0.0090
0.0207	0.0207	0.0207	0.0207	0.0207
0.0395	0.0395	0.0395	NaN	NaN

Some important conclusions can be made by looking at this experiment. First of all one can conclude that a Gaussian distribution of errors in the measured strain indeed results in a Gaussian distributed error in the calculated forces. As can be seen in table 3, the standard deviation of the error in the calculated F_x and F_y are both equal to the standard deviation of the error in the strain.

Another big conclusion that can be drawn has to do with the expression 'NaN', which can be found in table 3. When adding errors to the strains, the method of Newton-Raphson does not always lead to a proper result. When these errors are too big, the solution will not converge, but diverge leading to a singular matrix. In those cases the problem cannot be solved. When this happens in real life, the problem can be fixed by adjusting the initial guesses. During the simulations this is not possible with as effect that in those cases the standard deviation is not a number (NaN). To increase the robustness of the Newton-Raphson algorithm, regularization as suggested in [2] is applied. However, this still led to a singular matrix in some cases. Even if one works with larger numbers in this experiment, a singular matrix can result. When errors are getting bigger, one must thus rely on the least square method.

In real life it is very unlikely that all strain gauges have the same error in a measurement. That is why it is better to give all sixteen strains a different error, determined by the same Gaussian distribution. Again, if the errors in the strain are normally distributed, the resulting errors in the forces are normally distributed too. However, in this case the resulting standard deviations cannot be explained easily. If the error is only in gauges one to eight, there will be only an error in the calculated F_y . The standard deviation of this calculated force is no longer equal to the one of the error in the strain, but they are linearly related. The same holds for errors in gauges nine to sixteen with respect to F_x . If all gauges have an error, we get the combined situation of above.

In this situation a new problem arises: the standard deviations in the calculated forces are dependent on the ratio between F_x and F_y . This does not come as a surprise, since F_x and F_y have different relations with the sixteen strains. If both forces become twice as large, the standard deviations in the calculated forces stay the same. However, if only one of the two forces changes, the standard deviation of the error in this changed, calculated force will also change. In the realistic case of sixteen different errors, a more accurate sensitivity analysis is needed to draw conclusions on the effect of errors in the measurement on the calculated forces. When all sixteen errors are the same, one can conclude that using the least square method the applied forces are calculated within the accuracy of the measurement instruments.

5.2 Error in grid

Another situation to examine is the one in which the coefficients of the grid are incorrect. The grid is namely determined using ANSYS and the values will thus always differ from reality. To this end, the assumption is made that the strain gauges measure correctly. Again, all coefficients of the grid are first multiplied with the same error, being an error determined from a Gaussian distribution. The percentages that are used are the same as in the previous section. This experiment is repeated 2000 times and as can be seen below for a standard deviation of 0.01, the error in the calculated forces is also normally distributed.

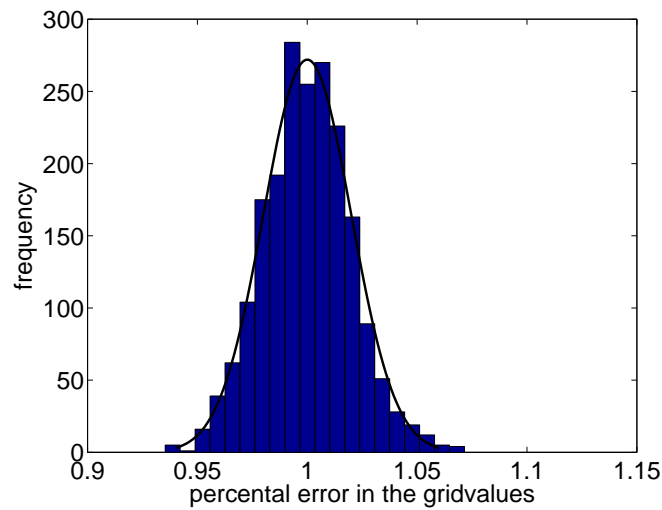


Figure 16: Normal distributed error in grid values

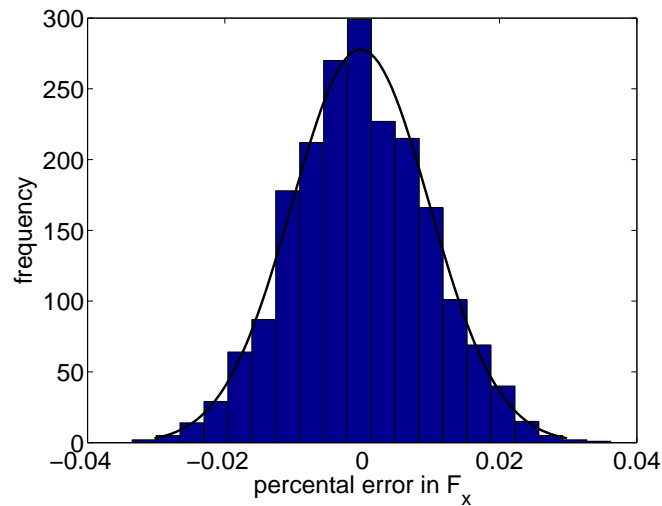
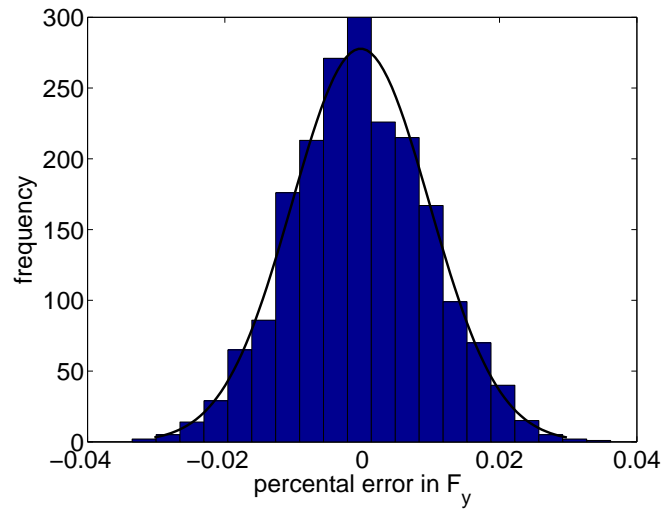


Figure 17: Normal distributed error in F_x

Figure 18: Normal distributed error in F_y

When repeating this for different standard deviations, again a table of the results is made.

Table 4: Standard deviations of calculated forces for a constant grid error

$\sigma(\text{error grid})$	$\sigma(\text{error } F_x)$ Least square	$\sigma(\text{error } F_y)$ Least square	$\sigma(\text{error } F_x)$ Newton-Rap.	$\sigma(\text{error } F_y)$ Newton-Rap.
0.0100	0.0100	0.0100	0.0100	0.0100
0.0192	0.0191	0.0191	NaN	NaN
0.0391	0.0394	0.0394	NaN	NaN

The conclusions that can be drawn here are the same as in the previous section. If all coefficients have the same normally distributed error, the calculated forces will also have a normally distributed error, with the same standard deviation as the one of the error in the coefficients of the grid. Again, when using the method of Newton-Raphson, the expression 'NaN' appears if the errors become too big. It is very unlikely that the error in all coefficients will be equal. That is why a second experiment is done, in which all coefficients of the grid have a different error.

Again one can conclude that a Gaussian distribution of an error in one of the inputs, in this case the coefficients of the grid, leads to a Gaussian distribution of the errors in the calculated forces. The standard deviation of the error in the calculated forces is again dependent on the ratio of the forces and linearly related to the standard deviation of the errors applied on the grid. A larger and more accurate sensitivity analysis is needed to say more about the effect of errors in the coefficients of the grid.

When all grid coefficients have the same error, the least square method calculates the applied forces within the accuracy of the errors in the grid.

5.3 Combining errors

The worst-case scenario is of course the situation in which both the strains and the grid-coefficients are incorrect. This is also tested in two steps. First, both all strains and all grid coefficients are multiplied with the same Gaussian distribution with average 1 and standard deviation of 1, 2 and 4 percent. The results of this experiment can be found in the table below.

Table 5: Standard deviations of calculated forces for a constant error in grid and strains

$\sigma(\text{error})$	$\sigma(\text{error } F_x)$ Least square	$\sigma(\text{error } F_y)$ Least square	$\sigma(\text{error } F_x)$ Newton-Rap.	$\sigma(\text{error } F_y)$ Newton-Rap.
0.010	0	0	$1.64e^{-11}$	$9.01e^{-12}$
0.020	0	0	$1.62e^{-11}$	$8.61e^{-12}$
0.0397	0	0	$1.62e^{-11}$	$8.87e^{-12}$

As can be seen, the errors cancel out if all inputs have the same error. In this situation, both methods calculate the applied forces correctly. Again, and this is perhaps the most interesting scenario, all inputs will be given a different error within this Gaussian distribution. In that case it is again impossible to find an expression for the standard deviation of the error in the calculated forces. Experiments do show that this standard deviation is linearly related to the standard deviation of the applied errors and that it is dependent on the size of the applied forces. If one wants to find a trend, a more accurate and more expanded sensitivity analysis is needed.

6 Experiments

The beam, with dimensions as determined in section 3.2, is produced and can be used for testing. However, due to time reasons, a simplification is made. In the test set-up, only vertical forces are considered and therefor only strains 1 to 8 will be measured. The beam is prepared and calibration takes place, after which the actual testing can be done.

6.1 Preparation of the beam

The gauges that will be used in our experiments are the gauges of figure 19. The gauge consists of three numbered sensors. All three sensors can measure a strain, but in a different direction. In our case the strains under an angle of 45 degrees must be measured, which is why parts 1 and 3 are used. Since only vertical forces are considered, four gauges are needed. Gauge 1 measures strains 1 and 2, gauge 2 measures strains 3 and 4, etcetera.

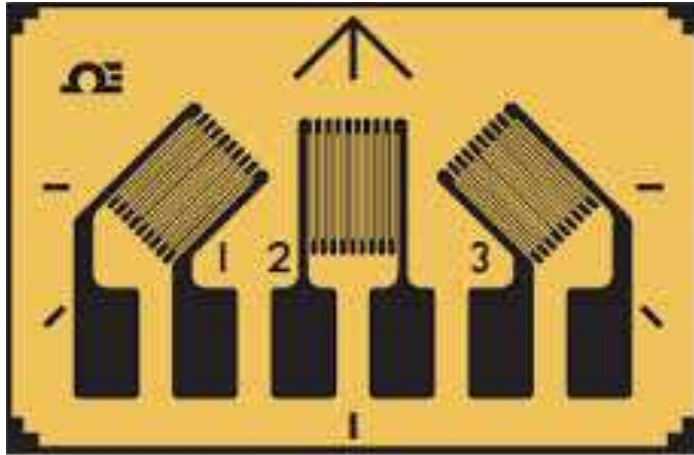


Figure 19: Illustration of the strain gauges used

Before the beam can be used for testing, several steps need to be done to prepare the beam. Some of these steps have a huge influence on the resulting accuracy, so it is of importance that these steps are handled with care. First of all, the position of the gauges needs to be determined. The gauges are mounted at the central axis, so at a height of 30 millimeters from the top. One gauge is placed at $1/4$ of the length of the beam, which is 100 millimeters from one end, and another gauge is placed at $3/4$ of the length of the beam, which is 300 millimeters from this same end. The height is determined with a tool which measures distance with an accuracy of 0.005 millimeters, while the distance in horizontal direction is found using a ruler with an accuracy of 0.5 millimeters. The same is done to place two gauges at the other side of the beam.

Around the exact position for the strain gauges, the surface is prepared. This consists of removing the paint and sanding the surface. After this, the surface is cleaned using acetone. The four gauges are then glued on the surface of the

beam, together with a pad. After this, wires are soldered from the gauges to their corresponding pads. The wires used here are as thin as possible. To keep the measurement error as low as possible, one should use as less wire as possible. Furthermore it is desirable that wires are close together and that they have the same length. When all gauges are connected to their pads, the pads must be connected in a correct way. To this end, one must first know the Wheatstone bridge.

6.2 Wheatstone bridge

The Wheatstone bridge is an electrical circuit which consists of four resistances. A current V_{in} is applied and between two points a current V_{out} is measured, as can be seen in the next picture.

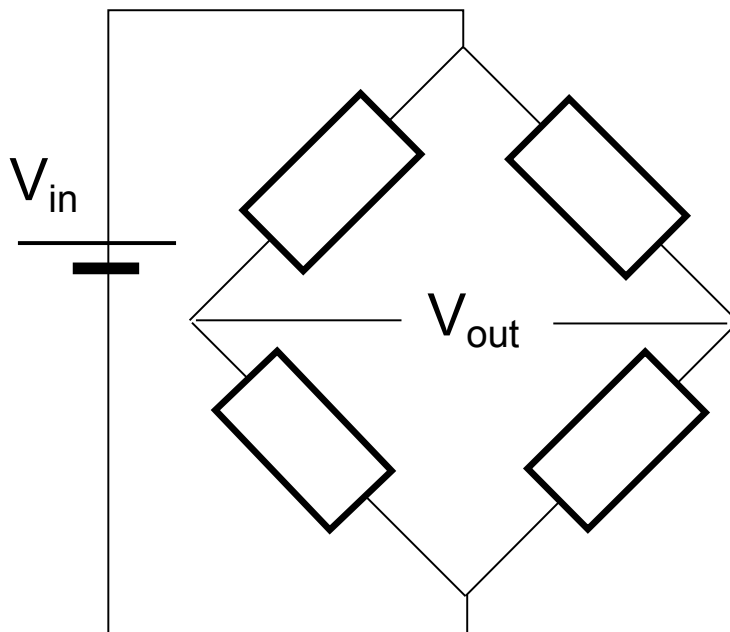


Figure 20: Basic Wheatstone bridge

When applying a known voltage V_{in} , one can measure the output voltage V_{out} , which clearly is dependent on the four resistances. In our case these are the resistances of the strain gauges, which are related to the strain in the beam and thus related to the applied force. When using the full-bridge configuration, which means that all four elements in figure 20 have a varying resistance, the output voltage is directly proportional to the applied force.

To find out where to attach which gauge, one must look back at formula 20, derived earlier, in section 2.3. This formula relates the eight strains with the applied load in the following way:

$$P \sim e_1 + e_4 + e_5 + e_8 - e_2 - e_3 - e_6 - e_7. \quad (45)$$

Since in this case eight strains are measured, each element in the basic Wheatstone bridge of figure 20 must consist of two sensors. To this end, each element is the summation of the resistances of two sensors with the same configuration, but both on a different side of the neural axis. This way the resistances of sensors 1 and 5 are added, as well as the resistances of sensors 2 and 6, 3 and 7 and 4 and 8.

To decide which sensor needs to be placed where in this circuit, one requirement of [1] must be met. When looking at figure 20, all adjacent elements must have a different sign (tension or compression) from their neighbours. Keeping this requirement in mind and using the numbering of strains 1 to 8 again, the final configuration of the Wheatstone bridge is depicted below.

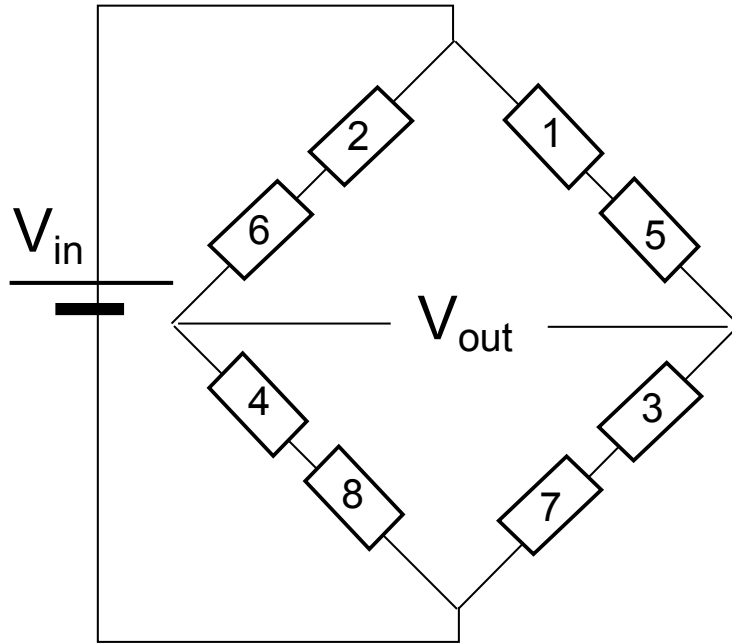


Figure 21: Wheatstone bridge for our test set-up

The output voltage is, as stated earlier, in this case linearly relate to the applied force. The relationship between the output voltage and the eight strains is the following:

$$V_{out} = GE * \frac{1}{4} * F_g * \left(\frac{e_1 + e_5}{2} + \frac{e_4 + e_8}{2} - \frac{e_2 + e_6}{2} - \frac{e_3 + e_7}{2} \right). \quad (46)$$

In this equation GE is a constant which depends on the input voltage and the values of the amplifier. F_g is the Gauge Factor and this factor tells something about the change in resistance of a gauge due to strain. With our grid as derived in section 4.1, one can find all eight strains when the applied force and its position is known. In this way a relation is found to calculate the expected output voltage from an applied known force.

The constant GE can be found by using the amplifier. When one is sure it is warmed up, the output voltage when no strain is applied, can be registered. Then, on the amplifier a strain is applied, which is in the same order of magnitude as the strain in the final tests. The new output voltage is registered and the difference between this voltage and the initial value of the output voltage is called δV . With this difference the value of GE can be determined using

$$GE = \frac{\delta V * 4}{F_g^* * \epsilon}. \quad (47)$$

In this equation F_g^* is the theoretical value of the Gauge Factor and ϵ the applied strain.

Only in case of so called 'balancing legs', when $\frac{R_1}{R_2} = \frac{R_3}{R_4}$ when the system is in rest, equation 46 initially leads to an output voltage of zero. However, with the amplifier used, one can set the initial output voltage to zero even if the resistances are not 'balancing'.

6.3 Calculate Force-Voltage curve

Using our predefined grid and equation 46, one can determine how the eight strains are related to the applied force. When a vertical force is applied in the middle of the beam, these relations are as follows:

$$\begin{aligned} e_1 &= 1.0297e^{-9} * F \\ e_2 &= -1.8272e^{-9} * F \\ e_3 &= -1.8272e^{-9} * F \\ e_4 &= 1.0297e^{-9} * F \\ e_5 &= 1.0293e^{-9} * F \\ e_6 &= -1.8249e^{-9} * F \\ e_7 &= -1.8249e^{-9} * F \\ e_8 &= 1.0293e^{-9} * F \end{aligned}$$

Furthermore the value of GE is determined. When not applying any strain on the amplifier, the output voltage is 45 mV. When applying a strain of $60 e^{-6}$, the output voltage is 1252 mV. This means that δV is equal to 1207 mV and when using the theoretical value of the Gauge Factor, which is 2.00, equation 47 leads to a value of 40233.33 for GE . The actual Gauge Factor is given by the fabricator and for these gauges it is 2.01 +- 1%.

When all these values are known, equation 46 can be used to determine the theoretical relation between an applied force and the output voltage. This is also done for forces applied at positions $z=0.016$ and $z=0.044$. As can be seen in the picture below, this relation is linear with a slope of $1.15e^{-4}$ and is independent of the position where the force is applied.

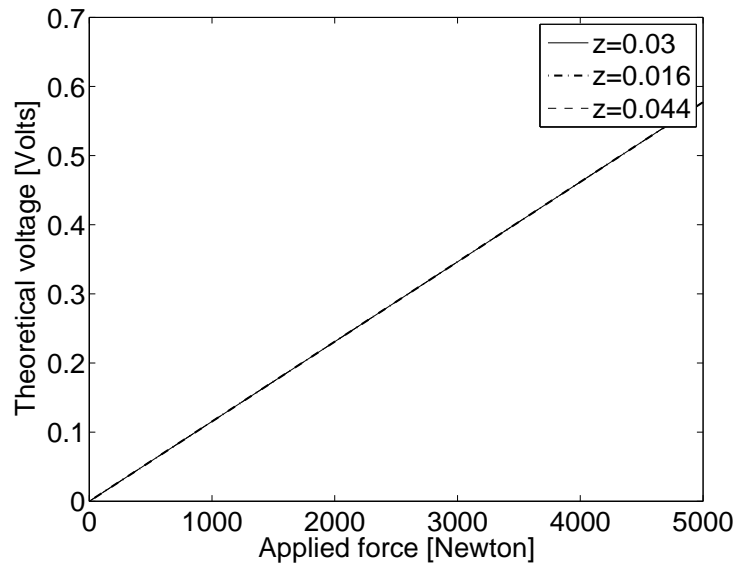


Figure 22: Theoretical relation between applied forces and output voltages for different positions

6.4 Results

Before starting measuring, all equipment is connected in a proper way and some time is taken to let the equipment get warm. When the initial output voltage reaches a stable value, measurements can be started. A press is used to exert forces on the beam. Since this press consists of a large surface through which force is applied, an extra aluminium rod is used to make sure the force is only applied at a small part of the beam, namely the middle of the beam. The force is increased from 0 to 20.000 Newton and every 2000 Newton the voltage is registered. The results of this first test can be found in the table below.

Table 6: Measured output voltage for an applied force

δF [N]	F [N]	U [mV]
0	0	117
2071	2071	327
2102	4173	529
2113	6286	707
2007	8293	780
1960	10253	786

At a force of 10.253 Newton the experiment is stopped. One can see that in the first two steps the voltage increases linearly with ± 200 mV. When applying 8000 Newton the meter shows a voltage of around 930 mV, but then directly drops down to 780 mV. One assumption is that this is due to the plastic deformation of the aluminium rod. That is why this rod is replaced for an iron rod and the experiment is repeated. However, the same effect occurs.

It turns out that when applying forces larger than 5000 Newton, the press has problems to keep this force applied for a time long enough to register the voltage. When the right force is reached the machine 'relaxes' and retracts a bit, leading to a lower force and thus a lower voltage. This is why the experiment is continued for forces up to 5000 Newton, with a stepsize of 1000 Newton. This procedure is repeated three times with the force applied in the middle of the beam. After this, the procedure is repeated three times when applying the force at the left and right side of the middle of the beam. The averages of three measurements at each position are depicted below. All data can be found in Appendix B.

Table 7: Average output voltages for an applied force at different positions

F[N]	U(z=0.03) [mV]	U(z=0.016) [mV]	U(z=0.044) [mV]
0	111.0	111.0	111.0
1001	216.3	217	215.7
2002	318.7	322	318.3
3003	420.7	424.7	419.7
4004	520.7	525	517.7
5005	615.3	622.3	612.3

For each position a graph is drawn. In this graph the measurement data and a line that fits these data best is plotted, together with the theoretical values. The next three figures show the results from measurements at $z=0.03$ m, $z=0.016$ m and $z=0.044$ m respectively.

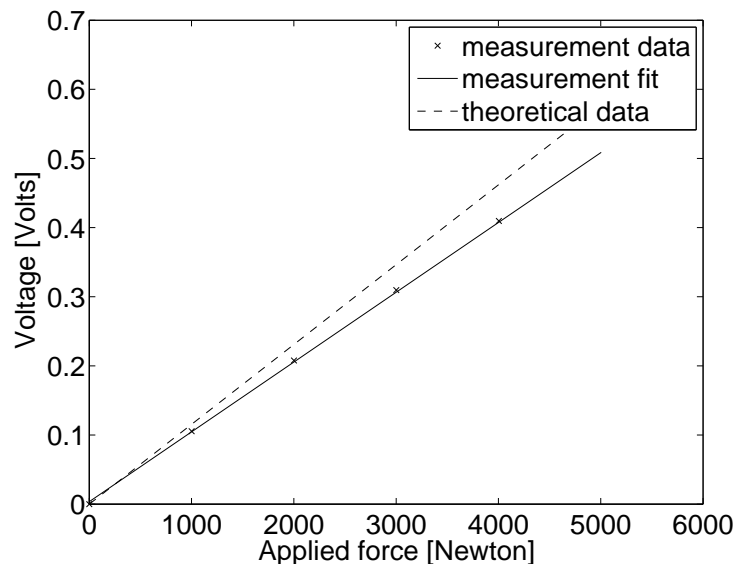
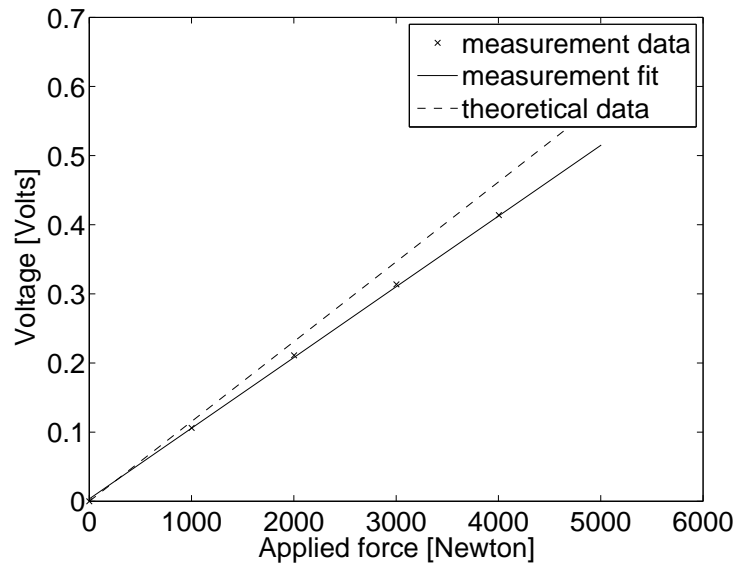
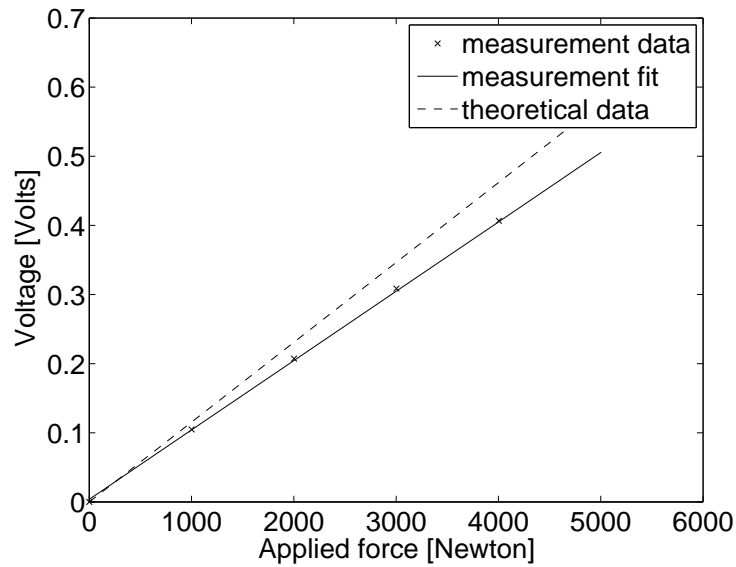


Figure 23: Theoretical and experimental results compared for $z=0.03$

Figure 24: Theoretical and experimental results compared for $z=0.016$ Figure 25: Theoretical and experimental results compared for $z=0.044$

One can clearly see that the experimental relation is indeed linear, but that the slope of the experimental lines is a bit different from the theoretical values. Since during testing the initial offset equaled 0.111 Volts, all test data are subtracted with 0.111 Volts, so they can be compared with the theoretical model.

Also a fourth graph is drawn, which is the experimental version of figure 22.

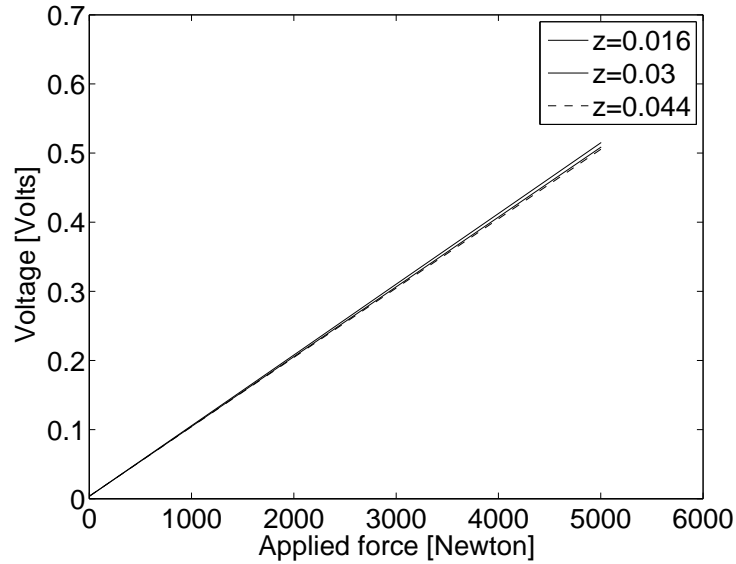


Figure 26: Experimental results for different positions compared

As can be seen in figure 26, the experimental curves defer a little bit when the load is not exactly applied in the middle. This can be seen best when looking at high forces. Since all the measurements had the same initial output voltage, there is no problem with the 'warming-up' of the equipment. However, the change in curves could be due to an error in the positioning of the gauges. Probably one or more of the gauges is not placed exactly horizontal, leading to strains that are not exactly under an angle of 45 degrees, resulting in different results when the force is applied elsewhere.

Furthermore the computer displays the displacement of the beam, which, for an applied force of 5000 Newton, is around 0.1 mm. Calculations in section 3.3 showed a displacement of 0.125 mm at this force, so this is another sign that our model corresponds to the actual situation.

7 Conclusion

The goal of this research was finding a way to measure contact forces of train wheels with the track. To this end a new force sensor had to be designed. A circular beam is designed with dimensions such that it fits the bottom profile of the train wheel and such that the Yield strength of the material is not exceeded when vertical forces up to 20.000 Newton are applied. This condition is also checked using ANSYS. Both vertical and horizontal forces that are exerted on the beam lead to deformations in the beam, which can be measured.

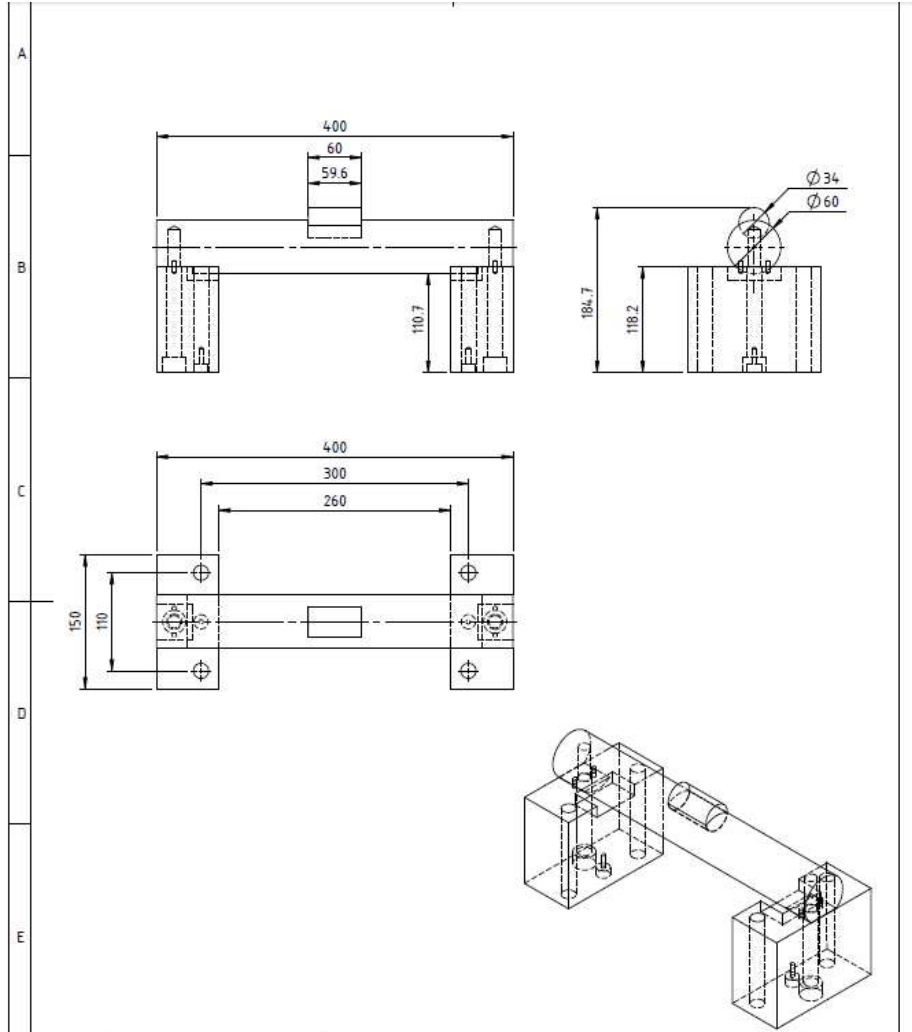
To this end, sixteen strains need to be measured, all under an angle of 45 degrees with the neutral axis. The theoretical relation between these strains and the applied forces is determined and two algorithms are made for calculating the applied forces from the measured strain, when the position of application is unknown. To this end a grid is applied on the small cylinder and some reference data is needed. The resulting set of equations can be solved either by using the method of minimizing the error or by using Newton-Raphson iteration. Both procedures are tested and verified using the model in ANSYS.

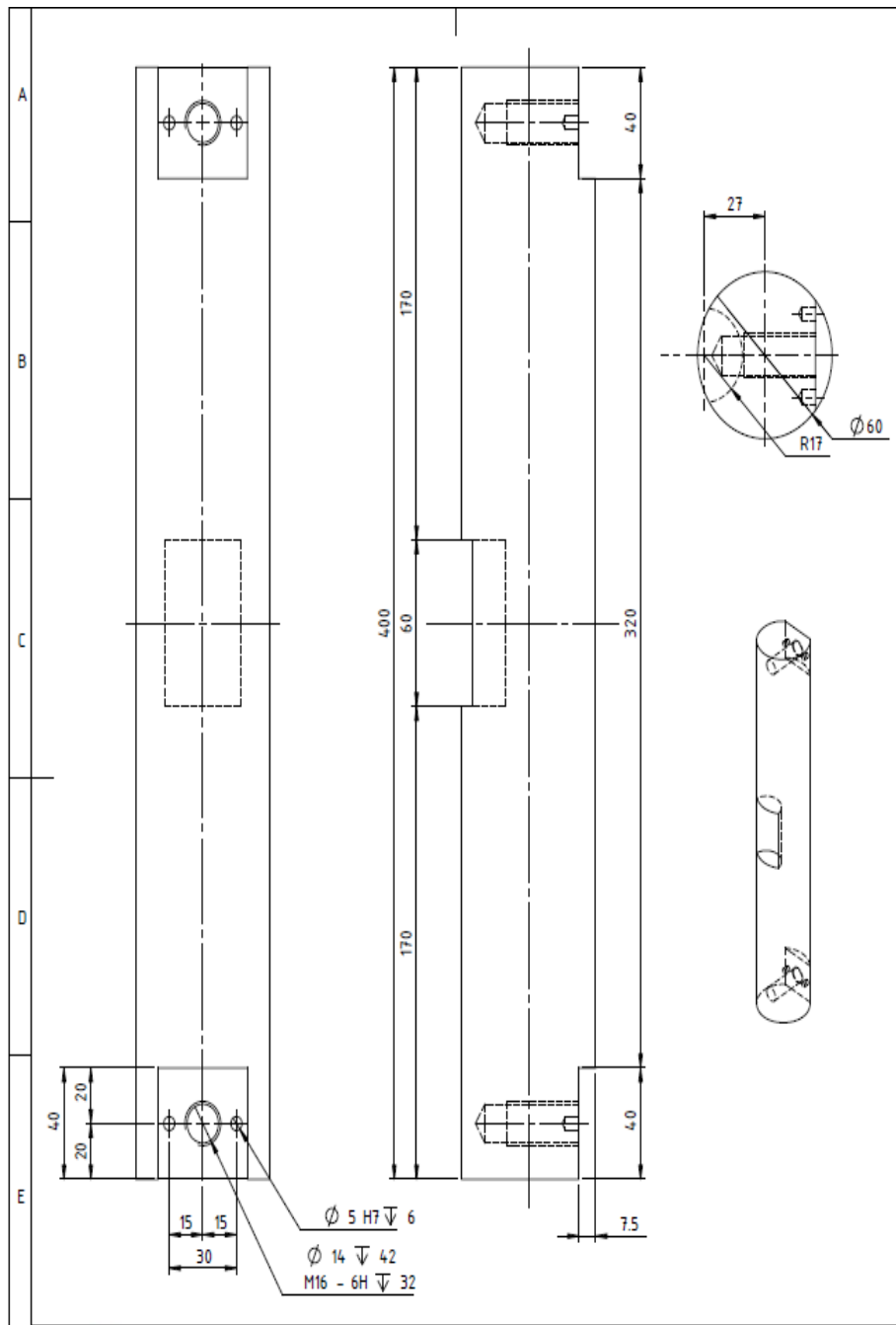
The sensitivity analysis showed that the method of Newton-Raphson does not work properly when there are errors in the measurement or in the tools. When using the method of minimizing the error, it turned out that an error in the measured strain effected the calculated force. If all strain gauges have the same error, this exact error will also be in the calculated forces. When all gauges have a different, normal distributed error, the error in the calculated forces is also normally distributed, where the standard deviation is dependent on the size of the forces. The same holds for errors in the values of the grid.

For experimenting, the problem is adapted and the beam only needs to measure vertical applied forces. When working with a Wheatstone bridge, the output voltage should be linearly related to the applied force. It turned out that this was the case, but that the slope was different from the theoretical value. Furthermore the slope was dependent on the position where the force is applied, which tells that the placement of the gauges is not perfect.

A further research could have as goal to indeed test the actual algorithm. In that case all 16 strains should be registered. These strains could then be used to solve our set of equations by minimizing the error. In that case a combination of a horizontal and vertical force could be applied somewhere along the small cylinder. Also the same beam could be tested again after replacing the strain gauges, to see if the error is indeed due to the misplacing of the gauges. Furthermore one could examine how to make the method of Newton-Raphson more robust. A final possibility for further examination is to perform a larger and more accurate sensitivity analysis.

A Dimensions of the beam





B Test data

Table 8: Measured output voltage for an applied force at $z=0.03$

δF [N]	U1 [mV]	δF [N]	U2 [mV]	δF [N]	U3 [mV]
0	111	0	111	0	111
1000	216	1001	216	1001	217
1001	318	1000	318	1000	320
1001	420	1001	419	1001	423
1002	520	1002	518	1001	524
1002	615	1002	612	1000	619

Table 9: Measured output voltage for an applied force at $z=0.016$

δF [N]	U1 [mV]	δF [N]	U2 [mV]	δF [N]	U3 [mV]
0	111	0	111	0	111
1001	217	1002	217	1000	217
1002	321	1002	322	1000	323
1001	423	1000	424	1001	427
1002	522	1001	526	1001	527
1001	619	1001	624	1000	624

Table 10: Measured output voltage for an applied force at $z=0.044$

δF [N]	U1 [mV]	δF [N]	U2 [mV]	δF [N]	U3 [mV]
0	111	0	111	0	111
1001	215	1002	216	1002	216
1000	315	1001	320	1002	320
1001	414	1001	423	1001	422
1001	512	1000	520	1000	521
1003	605	1001	615	1001	617

References

- [1] Karl Hoffman, *Applying the Wheatstone Bridge Circuit*.
- [2] Michiel E. Horstenbach and Lothar Reichel, *An iterative method for tikhonov regularization with a general linear regularization operator*, June 2010.
- [3] Warren C Young, *ROARK'S Formulas for stress and strain*, Mc-Graw-Hill Book Co., 6th International Edition, 1989.
- [4] National Model Railroad Association, 2002, <http://www.nmra.org/beginner/wheelsets.html>.
- [5] Positioning strain gages to monitor bending, axial, shear, and torsional loads, 2003, <http://www.omega.com/faq/pressure/positioning>.
- [6] 60 degrees Delta Rosette Strain Gauge Planar Geometry, 2003, <http://www.omega.nl/pptst.html>.